MCB
Journals.ASM.org

Overexpression of Epigen during Embryonic Development Induces Reversible, Epidermal Growth Factor Receptor-Dependent Sebaceous Gland Hyperplasia

Maik Dahlhoff,[a] Daniela Frances,[b] Jennifer E. Kloepper,[f] Ralf Paus,[d,g] Matthias Schäfer,[e] Catherin Niemann,[b,c] Marlon R. Schneider[a]

Gene Center, LMU Munich, Munich, Germany[a]; Center for Molecular Medicine Cologne, University of Cologne, Cologne, Germany[b]; Center for Biochemistry, Medical Faculty, University of Cologne, Cologne, Germany[c]; Institute of Inflammation and Repair, University of Manchester, Manchester, United Kingdom[g]; Department of Dermatology, University of Muenster, Muenster, Germany[d]; Institute of Molecular Health Sciences, ETH Zurich, Zurich, Switzerland[e]; Department of Dermatology, University of Lübeck, Lübeck, Germany[f]

The epidermal growth factor receptor (EGFR) system is a key regulator of epithelial development and homeostasis. Its functions in the sebaceous gland (SG), however, remain poorly characterized. In this study, using a transgenic mouse line with tissue-specific and inducible expression of the EGFR ligand epigen, we showed that increased activation of the EGFR in skin keratinocytes results in enlarged SGs and increased sebum production. The phenotype can be reverted by interrupting transgene expression and is EGFR dependent, as gland size and sebum levels return to normal values after crossing to the EGFR-impaired mouse line Wa5. Intriguingly, however, the SG enlargement appears only if EGFR activation occurs before birth. Importantly, the enlarged sebaceous glands are associated with an increased expression of the transcription factor MYC and of the transmembrane proteins LRIG1, an established negative-feedback regulator of the EGFR/ERBB tyrosine kinase receptors and a stem cell marker. Our findings identify EGFR signaling as a major pathway determining SG activity and suggest a functional relationship between the EGFR/ERBB system and MYC/LRIG1 in the commitment of stem cells toward specific progenitor cell types, with implications for our understanding of their role in tissue development, homeostasis, and disease.

The mammalian skin serves as a barrier to avoid water loss and to protect against physical, chemical, and biological environmental hazards. As for other tissues with high epithelial cell turnover, the skin depends on stem cells (SCs) to maintain its integrity throughout life and to regenerate upon injury. In fact, multiple SC populations contribute with various degrees of overlap to the homeostasis and repair of the different compartments of the skin, the interfollicular epidermis (IFE) and appendages such as hair follicles (HFs), sebaceous glands (SGs), and sweat glands (1–5).

While the exact details are still under study (6), the renewal of the IFE during homeostasis follows a rather simple pattern in that SCs in the basal layer generate daughter cells that, while initially mitotically active, soon undergo a terminal differentiation program as they exit the cell cycle, migrate upwards, and progressively contribute to all epidermal layers (7). In contrast to the continuous nature of epidermal renewal, the HF undergoes repeated cycles of growth (anagen), involution (catagen), and relative rest (telogen) (8–10). Follicular growth during anagen depends on the activation of SCs located in the bulge, a permanent part of the HF located below the SG where the arrector pili muscle inserts into the outer root sheath (11). The identification of keratin 15 (12, 13) and CD34 (14) as suitable markers of murine bulge cells allowed lineage tracing and transplantation experiments, revealing that these cells have the potential to contribute to the IFE, HF, and SG lineages (15, 16). Genetic lineage tracing studies also demonstrated that bulge SCs do not contribute to IFE homeostasis but can be mobilized to regenerate this compartment following injury (17–19).

During the last decade, a considerable number of SC populations have been identified at different positions of the pilosebaceous unit in addition to the bulge. In the lower bulge region, extending to the hair germ, a group of LGR5-positive cells actively proliferate at the beginning of anagen and can contribute to all regions of the HF (20). A number of distinct SC populations have also been localized in the isthmus, the region immediately below the SG, and in the junctional zone, which represents the area around the opening of the SG into the hair canal. These SC populations can be identified by the expression of LGR6 (21), MTS24/PLET1 (22, 23), LRIG1 (24), and BLIMP1 (25).

Studies based on lineage tracing or marker localization revealed that the SG, an epidermal appendage that produces sebum via holocrine secretion (26, 27), can be formed by committed cells derived from different SC populations, including BLIMP1$^+$ cells (25), LGR5$^+$ cells (20), LGR6$^+$ cells (21), and LRIG1$^+$ cells (24, 28). However, formation of SGs by bulge-derived cells has also been reported (15, 16, 18, 29). Thus, the SC type fueling SG turnover remains disputed.

Recently, we reported greatly enlarged SGs in transgenic mice with ubiquitous expression of epigen (EPGN) (30). EPGN is a ligand of the epidermal growth factor receptor (EGFR) with several unique features, such as persistent and potent biological actions in spite of low receptor binding affinity (31, 32). While histological analyses carried out with EPGN-expressing transgenic

Received 3 March 2014 Returned for modification 1 April 2014
Accepted 27 May 2014
Published ahead of print 2 June 2014
Address correspondence to Marlon R. Schneider, marlon.schneider@lmu.de.
Supplemental material for this article may be found at http://dx.doi.org/10.1128/MCB.00302-14.

doi:10.1128/MCB.00302-14

founders revealed increased sebocyte proliferation as the underlying cause for the increased gland size in these mice, the widespread expression of the transgene, which resulted in infertility, precluded detailed mechanistic analysis. In this study, we generated a transgenic mouse line with skin-specific, inducible expression of EPGN and employed it to study the functions of this EGFR ligand in the skin, with particular attention to its role in the SG and its influence on various epithelial SC populations.

MATERIALS AND METHODS

Animals. Mice were maintained under specific-pathogen-free conditions and had access to water and standard rodent diet (V1534; Ssniff, Soest, Germany) *ad libitum*. All experiments were approved by the Committee on Animal Health and Care of the local governmental body of the state of Upper Bavaria (Regierung von Oberbayern), Germany, and were performed in strict compliance with the European Communities Council Directive (86/609/EEC) recommendations for the care and use of laboratory animals.

Egfr$^{Wa5/+}$ mice (Wa5) expressing an antimorphic *Egfr* allele (33) were donated by the Medical Research Council (Oxfordshire, United Kingdom). For generating K14-EPGN mice, we first cloned human *EPGN* cDNA (kindly provided by Yosef Yarden, The Weizmann Institute of Science, Israel), into the pTRE-Tight vector (Clontech). After excision of the relevant sequences with XhoI, the construct was employed to generate two independent pTRE-Tight-EPGN transgenic mouse lines by pronuclear microinjection (FVB/N background). These mice were mated to a K14-rtTA mouse line (34) to generate doubly transgenic animals (K14-EPGN). Addition of doxycycline (Dox, 3 mg/ml, and 50 mg/ml of sucrose; Sigma, Deisenhofen, Germany) to the drinking water of pregnant females resulted in skin-specific expression of epigen as increased coat greasiness in the doubly transgenic offspring of both lines. Therefore, we chose one line (L1) for carrying out all further studies. Epidermal sebum levels were measured with a Sebumeter (SM810; Courage and Khazaka, Cologne, Germany). For the evaluation of hair types, shafts were plucked from the backs of K14-EPGN and control mice and examined on microscope slides (100 hairs per animal, 3 mice per genotype).

RNA expression analysis. Back skin samples were homogenized in TRIzol (Invitrogen, Karlsruhe, Germany) for RNA isolation, and 1 μg of RNA was reverse transcribed in a final volume of 40 μl using RevertAid reverse transcriptase (Thermo Scientific, Schwerte, Germany) according to the manufacturer's instructions. For qualitative mRNA expression of human *EPGN*, reverse transcription-PCR (RT-PCR) using reagents from Qiagen (Hilden, Germany) was performed. The final reaction volume was 20 μl, and cycle conditions were 94°C for 5 min followed by 35 cycles of 94°C for 1 min, 60°C for 1 min, and 72°C for 1 min. The primers employed were human *EPGN* forward primer 5′-TTTGGGAGTTCCAATATCAG C-3′ and reverse primer 5′-TGTGATTGGAGGTGTTACAGTCA-3′ and *Gapdh* forward primer 5′-TCATCAACGGGAAGCCCATCAC-3′ and reverse primer 5′-AGACTCCACGACATACTCAGCACCG-3′.

Quantitative mRNA expression analysis was performed by real-time quantitative RT-PCR (qRT-PCR) using the LightCycler 480 system and the LightCycler 480 Probes Master (Roche, Mannheim, Germany). The final primer concentration was 0.5 μM, and the probe concentration was 0.2 μM. The final reaction volume was 10 μl, and cycle conditions were 95°C for 5 min followed by 45 cycles of 95°C for 10 s, 60°C for 15 s, and 72°C for 1 s. Quantitative values are obtained from the threshold cycle (C_T) number, at which the increase in the signal associated with the exponential growth of PCR products begins to be detected. Transcript copy numbers were normalized to *Actb* mRNA copies. Results are expressed as fold differences in target gene expression relative to that of *Actb* transcripts. The ΔC_T value of the sample was determined by subtracting the average C_T value of the target gene from the average C_T value of the *Actb* gene. Probes were labeled with the reporter dye 6-carboxyfluorescein (FAM) at the 5′ end and the quencher dye 6-carboxytetramethylrhodamine (TAMRA) at the 3′ end. For each primer pair, we performed no-template control and no-RT control assays, which produced negligible signals with C_T values that were usually greater than 40. Experiments were performed in duplicates for each sample. Sequences of primers (Thermo Fisher Scientific, Dreieich, Germany) and probes (Roche) for the evaluated transcripts are shown in Table S1 in the supplemental material.

Histology, immunohistochemistry, immunofluorescence, and morphometric analysis. After euthanasia, skin samples were fixed in 4% paraformaldehyde (PFA; Sigma-Aldrich, Germany) or 95% ethanol with 1% acetic acid, dehydrated, and embedded in paraffin or directly snap-frozen in OCT medium and stored at −80°C. Hematoxylin and eosin (H&E)-stained sections were employed for histological analysis. For the detection of proliferating cells, immunohistochemical staining of Ki67 was performed. Briefly, sections were boiled for antigen retrieval in 10 mM sodium citrate buffer (pH 6.0), and the endogenous peroxidase was blocked with 3% H_2O_2 for 15 min. Slides were blocked with 5% rabbit serum and incubated overnight at 4°C with a rat anti-Ki67 antibody (Dako, Denmark) diluted 1/200. After being washed in Tris-buffered saline solution (TBS), the slides were incubated for 1 h with a secondary biotin-conjugated rabbit anti-rat antibody (Dako) diluted 1/200 and then for 30 min with streptavidin-biotin complex. 3,3′-Diaminobenzidine (KEN-EN-TEC, Denmark) was used as the chromogen.

Epidermal differentiation was investigated by immunofluorescence analysis. Briefly, acetic ethanol-fixed sections were blocked with 3% bovine serum albumin (BSA) in phosphate-buffered saline (PBS)–1% Tween (PBST) and incubated overnight at 4°C with rabbit anti-keratin 6 (1:1,000), anti-keratin 10 (1:500), anti-keratin 14 (1:50,000), or anti-loricrin antibody (1:250) (Covance, Berkeley, CA) in blocking solution. Afterwards, slides were washed with PBST and incubated with goat anti-rabbit Cy3 antibody (1:250) (Jackson ImmunoResearch, West Grove, PA) and Hoechst (1:1,000) (Sigma-Aldrich, Steinheim, Germany) in blocking solution for 2 h at room temperature. After being washed with PBS, the sections were mounted with Mowiol plus 10% 1,4-diazabicyclo[2.2.2]octane (DABCO) (Sigma-Aldrich).

Nile red staining was performed on 8-μm cryosections. Sections were fixed for 10 min in 4% PFA and washed twice for 5 min each in TBS. Slides were incubated with Nile red solution (1:100) (AdipoRed; Lonza, USA) for 10 min and thereafter washed twice for 5 min each in TBS. For LRIG1 staining, cryosections were incubated for 2 h at room temperature with the primary antibody (goat anti-LRIG1, no. AF3688; R&D Systems, Wiesbaden-Nordenstadt, Germany), washed, and incubated with an appropriate secondary antibody labeled with Alexa Fluor 488 (Dianova, Hamburg, Germany). All sections were mounted with Vectashield (Biozol, Eching, Germany) with 4′,6-diamidino-2-phenylindole (DAPI) and stored at 4°C.

For the quantitative evaluation of HF numbers, SG area and proliferation index, two different sections from the back skin of 8-week-old control and K14-EPGN transgenic males ($n = 4$/genotype) were stained with H&E. Pictures covering a length of 3.25 mm of epidermis were taken with a ×200 magnification lens using a Leica DFC425C digital camera (Leica Microsystems, Wetzlar, Germany) for each section, resulting in a total length of 6.5 mm of back skin per animal to be measured. The number of HFs was recorded and the area of all visible SGs was recorded with LAS software version 3.8.0 (Leica Microsystems) and employed to calculate the mean gland area. Epidermal thickness was investigated on the same sections on 10 constantly distributed measuring points per picture, resulting in a total of 150 measuring points per animal. For determining the proliferation rate, the total number of cells and the number of proliferating cells per sebaceous gland were determined on the same samples after staining for Ki67. To analyze the epidermal proliferation rate, the total number of epidermal nuclei and the total number of Ki67 positive nuclei were determined.

Electron microscopy. For electron microscopy, tail skin was immersed in 2.5% glutaraldehyde in Soerensen's phosphate buffer (pH 7.4) for 1 h. Soerensen's phosphate buffer was subsequently used to rinse the fixed tail skin. Samples with a length of 2 mm were cut and postfixed in 2%

OsO_4 for 2 h. Repeated Soerensen's phosphate buffer rinses and a graded alcohol series were carried out before the segments were embedded in epoxy resin. For electron microscopy, ultrathin sections (80 nm) were contrasted with uranyl acetate and lead citrate. Specimens were assessed via Zeiss-EM10 (Zeiss, Munich, Germany).

Histomorphometric analyses of hair follicle morphogenesis and hair follicle cycling. Quantitative histomorphometry was performed using morphological criteria to determine the different HF morphogenesis stages on postnatal days 0.5 (P0.5) and 8.5 (35) and the different HF cycle phases on postnatal day 18.5 (36). The hair morphogenesis and hair cycle score were calculated accordingly. The number of HFs in each specific morphogenesis stage or specific hair cycle phase was multiplied by the corresponding factor. The results of each sum were totaled and divided by the total number of HFs counted. This allows one to identify even subtle abnormalities in the dynamics of HF morphogenesis and cycling between test and control mice that might otherwise have escaped notice.

Whole-mount preparations and immunofluorescence. The harvest, processing, and immunofluorescence staining of epidermal whole mounts were done essentially as described previously (28). Primary antibodies for detecting the following proteins were used: LRIG1, goat, diluted 1:100 (R&D Systems); SOX9, rabbit, diluted 1:2,000, a kind gift of M. Wegner (37); and SCD1, rat, diluted 1:200 (Santa Cruz). 5-Ethynyl-2′-deoxyuridine (EdU) staining was carried out according to the instructions of the manufacturer (Invitrogen). Analyses of immunofluorescent signals were performed by confocal microscopy (Olympus IX81).

Statistical analysis. Quantitative RT-PCR values were related to the mean value of the control group and compared by Mann-Whitney U tests (Prism; GraphPad Software, San Diego, CA), and data are presented as box plots with medians. The remaining data were analyzed with Student's *t* test and are presented as means ± standard deviations (SD) unless otherwise indicated. A P value of <0.05 was considered statistically significant.

RESULTS

Skin-specific epigen expression from midgestation causes sebaceous gland enlargement. Using the TET-ON system, we created a mouse line in which the expression of EPGN is restricted to the skin, can be induced at different time points, and can be reversibly interrupted. For this purpose, we employed pronuclear microinjection to generate transgenic mice in which the human *EPGN* cDNA is located downstream of the TET-responsive promoter TRE-Tight (data not shown) and crossed these mice with K14-rtTA transgenic mice (34). Offspring carrying both transgenes were designated K14-EPGN (Tg) mice, while littermates carrying none or only one transgene were termed control mice (Co). We then tested whether transgene expression could be induced by doxycycline (Dox) in adult K14-EPGN mice. As shown in Fig. 1A, adding Dox to the drinking water readily resulted in the detection of transgene-derived *EPGN* transcripts in the back and tail skin of K14-EPGN mice already 24 h thereafter, while no *EPGN* transcripts could be detected in any organ of K14-EPGN mice not receiving Dox.

Having shown the functionality and specificity of our transgenic system, we first asked whether treating pregnant females with Dox to induce EPGN expression from embryonic day 11.5 (E11.5), long before epidermal stratification and HF morphogenesis take place, would promote SG enlargement as in mice with ubiquitous and constitutive expression of the ligand (30). K14-EPGN mice born from such females appeared indistinguishable from their control littermates during their first week of postnatal life but were easily recognized thereafter due to their greasy hair coat (Fig. 1B). Histological examination of H&E-stained (Fig. 1C) and Nile red-stained (Fig. 1D) skin sections of 8-week-old K14-EPGN mice constantly kept under Dox treatment from E11.5 revealed the presence of lipid-loaded, enlarged SGs. Transmission electron microscopy analysis confirmed the presence of significantly enlarged lipid droplets in the cytoplasm of the sebocytes (Fig. 1E).

Quantitative morphometry (38) showed that SGs in K14-EPGN mice were nearly 7 times larger than control glands (Fig. 1F). Quantification also revealed a significant increase in the number of cells per gland and in the number of proliferating cells per gland (Fig. 1F). Quantitative RT-PCR revealed a significant increase in transcripts encoding the sebocyte differentiation protein markers PLIN2, PPARG, SCD1, and MC5R (Fig. 1G). Reflecting the enlarged gland size of K14-EPGN mice, significantly increased lipid amounts were detected in the skin of 8-week-old K14-EPGN mice with a Sebumeter (Fig. 1H).

In addition to the SG, we also detected increased thickness and proliferation of the epidermis (Fig. 1I). Surprisingly, quantitative histomorphometry also identified an increase in the number of HFs per epidermis length unit in K14-EPGN mice compared to that in control animals (Fig. 1J). In contrast to the increase in HF density in adult animals, the HF morphogenesis (see Fig. S1A in the supplemental material) and the HF cycle induction (see Fig. S1B) were comparable between groups, and the same was true for the morphology and the relative abundance of different hair types plucked from the back skin (see Fig. S1C and D). As shown previously for transgenic mice with ubiquitous expression of EPGN (30), evaluation of the expression pattern of proteins specific for the differentiation program of the epidermal basal layer (keratin 14), suprabasal layer (keratin 10), cornified layer (loricrin), or an HF-specific marker (keratin 6) revealed no changes in the epidermal differentiation program of K14-EPGN transgenic mice (see Fig. S1E).

We conclude that epidermis and HF-specific expression of EPGN from middle gestation results in hyperplastic SGs, augmented sebum secretion, and increases in epidermal thickness and in the number of HF, therefore recapitulating the changes observed previously in mice with ubiquitous expression of the transgene.

Epigen-induced sebaceous gland enlargement is EGFR dependent. While EPGN has been described as an EGFR-specific ligand (32), it remains unknown to what extent its actions are mediated by EGFR/ERBB heterodimers. To evaluate whether the SG phenotype is EGFR dependent, we crossed K14-EPGN mice with $Egfr^{Wa5}$ mice (Wa5), a line in which a mutation in the tyrosine kinase domain of the EGFR results in a dominant negative receptor (33). Addition of Dox to the drinking water from E11.5 resulted in a drastic increase in sebum levels of K14-EPGN mice at 4 to 5 weeks of postnatal life, reaching values close to 100 $\mu g/cm^2$ at 8 weeks of age (Fig. 2A). In contrast, the sebum levels in control, Wa5, or K14-EPGN × Wa5 mice remained low (<5 $\mu g/cm^2$) during the whole period (Fig. 2A). Examination of H&E-stained skin sections (Fig. 2B) and quantitative morphometry (Fig. 2C) showed that SGs of K14-EPGN × Wa5 mice at 8 weeks of age were significantly smaller than those of K14-EPGN mice. These data indicate that the EGFR is required for the SG phenotype of K14-EPGN mice.

In fact, it has been previously shown that only ~10% EGFR activity is still present in Wa5 mice (33). Also, since a marked enlargement of SGs has also been reported for mice overexpressing the related tyrosine kinase receptor ERBB2 (39), the residual SG enlargement observed in K14-EPGN mice may be the result of

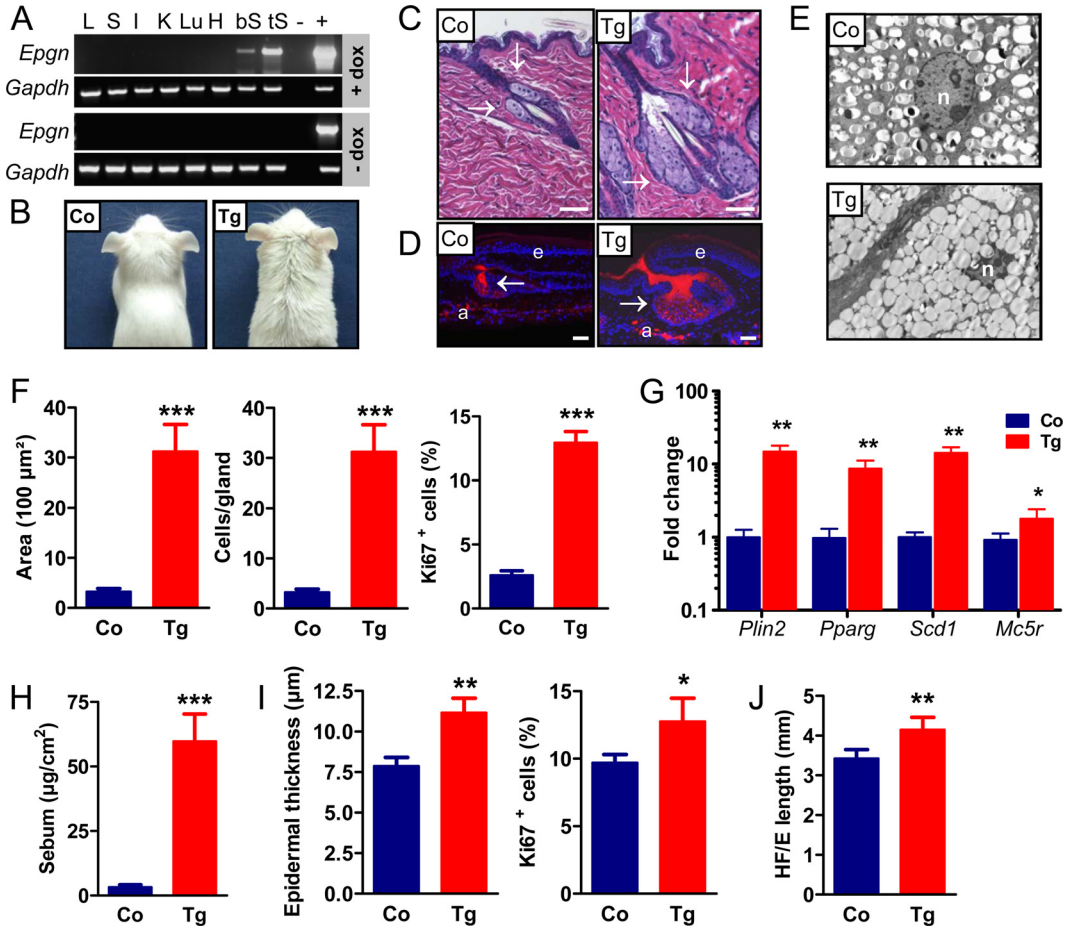

FIG 1 K14-EPGN transgenic mice show a Dox-inducible, reversible enlargement of the sebaceous gland. (A) RT-PCR shows Dox-dependent expression of transgene-derived *EPGN* in the back (bS) and tail (tS) skin of K14-EPGN mice. *Gapdh* amplification confirmed cDNA in all samples. L, liver; S, spleen; I, intestine; K, kidney; Lu, lung; H: heart. (B) Normal hair coat in control (Co) and oily hairs in K14-EPGN (Tg) mice. (C) H&E-stained back skin sections demonstrate enlarged sebaceous glands (arrows) in K14-EPGN (Tg) compared to control (Co) mice. (D) Nile red staining of tail skin sections confirmed increased lipid amounts in sebaceous glands (arrows) of K14-EPGN (Tg) compared to control (Co) mice. e, epidermis; a, dermal adipose tissue. (E) Electron micrographs demonstrate enlarged lipid droplets in the cytoplasm of sebocytes from K14-EPGN mice. n, cell nucleus. (F) Morphometric analysis of sebaceous glands showing significant increases in the mean gland area, in the number of cells/gland, and in the number of Ki67-positive nuclei/gland. Fifty individual glands were evaluated for every animal; 4 mice were used for each genotype. ***, $P < 0.001$. (G) qRT-PCR of skin mRNAs tested for the indicated sebocyte markers ($n = 5$ for each genotype). *, $P < 0.05$; **, $P < 0.01$. (H) Increased sebum levels in the skin of K14-EPGN (Tg) compared to control (Co) mice as evaluated by a Sebumeter ($n = 4$ mice/genotype). ***, $P < 0.001$. (I) Morphometric analysis of epidermal thickness and epidermal proliferation ($n = 5$ for each genotype). *, $P < 0.05$; **, $P < 0.01$. (J) Quantitative analysis of the HF number per mm of epidermis ($n = 4$ for each genotype). **, $P < 0.01$. Scale bars in panels C and D represent 100 μm.

EGFR/ERBB2 heterodimer activation by EPGN. Furthermore, the increase in epidermal thickness was completely rescued in Wa5 mice (Fig. 2D), additionally supporting our conclusion that epigen effects are mediated by the EGFR.

Sebaceous gland hyperplasia in K14-EPGN mice is dependent on continuous epigen supply. To evaluate whether the SG hyperplasia is dependent on continuous EPGN availability, we induced EPGN expression from E11.5 as described above and monitored skin sebum levels for several months. Sebum levels of K14-EPGN mice became significantly higher than that of control littermates from the third postnatal week and increased steadily, reaching values similar to those observed previously at 8 weeks of age (Fig. 3A). Removal of Dox from the drinking water after the 8th week of age caused a rapid decline in sebum levels, which reached values close to that of control mice after only 2 weeks (Fig. 3A). Notably, repeated administration of Dox or Dox withdrawal from the drinking water of these mice caused the sebum levels to rise or decline again, respectively (Fig. 3A). The changes in sebum levels during these cycles fully corresponded to changes in the SG size, as shown by quantitative evaluation of H&E-stained skin sections (Fig. 3B).

Sebaceous gland hyperplasia requires epigen activity before epidermal stratification. We next asked whether induction of EPGN expression at later stages of embryonic development or during postnatal life would result in an SG enlargement comparable to the one described above (from E11.5). When Dox treatment was initiated 2 days later (E13.5), K14-EPGN mice showed after birth an increase in skin sebum (Fig. 4A) and a greasy coat appearance (Fig. 4E) similar to those observed for mice receiving Dox from E11.5. However, postponing Dox administration to later stages such as E17.5, when epidermal stratification has taken place and the HFs are developing, resulted in signifi-

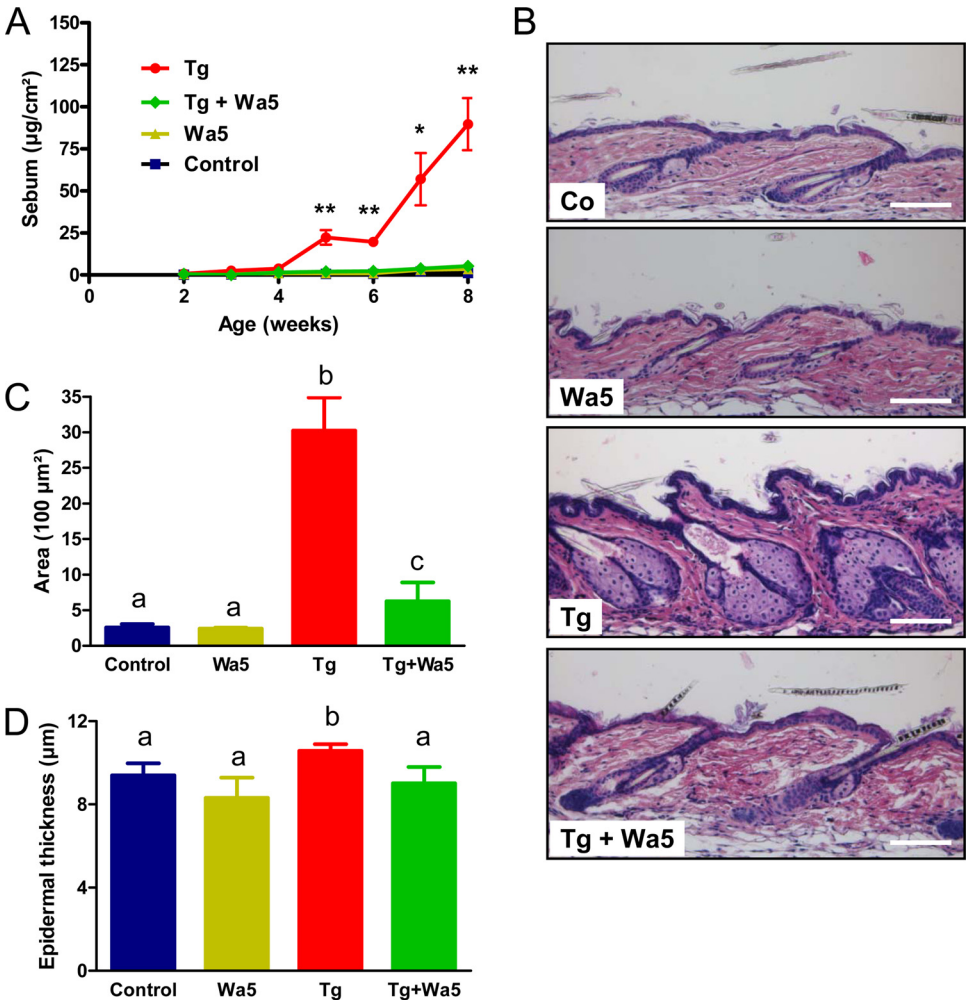

FIG 2 Introduction of the hypomorphic *Egfr* allele W5 largely rescues the sebaceous gland phenotype of K14-EPGN mice. (A) Evaluation of back skin sebum levels from early postnatal life to 8 weeks of age with a Sebumeter ($n = 5$ males/genotype). Error bars indicate SEMs. *, $P < 0.05$; **, $P < 0.01$. (B) Representative H&E-stained skin sections of 8-week-old mice of the indicated genotypes. Scale bars represent 100 μm. (C and D) Quantitative evaluation of sebaceous gland area (C) and epidermal thickness (D) in mice of the indicated genotypes at 8 weeks of age ($n = 5$ males/genotype). Different lowercase letters indicate statistically significant differences between groups (Student's *t* test). Data in panels C and D are means ± SD.

cantly lower sebum levels and milder coat phenotypes (Fig. 4B and E). When Dox administration was given at birth, the effects on sebum levels and coat appearance were even weaker (Fig. 4C and E). Notably, administration of Dox to adult K14-EPGN mice resulted in no changes in sebum levels or skin phenotype at all (Fig. 4D and E).

This intriguing observation suggests that increased epigen activity is required at an early stage of skin development in order to induce SG enlargement to its full extent, raising the question of how epigen impacts on defined subpopulations of SCs in the pilosebaceous unit, particularly on epithelial progenitor cells that give rise to sebocytes. The maintenance of SGs in adult skin has been attributed to a variety of SC populations (Fig. 5A). On the one hand, cells derived from the HF bulge region have been reported to renew the SG following injury or during skin homeostasis (15, 16, 18, 29). On the other hand, the SG may be replenished by progenitor cells located at the periphery of the gland (25, 40) or in the isthmus/junctional zone (21–24). Therefore, we next assessed changes in the expression of known epithelial HF SC markers in the skin of K14-EPGN to evaluate whether tissue-specific SCs contribute to the observed phenotype.

SG enlargement in K14-EPGN mice is associated with an expanded LRIG1$^+$ cell pool. Since the effect of transgene-derived epigen takes place around the time the epidermis stratifies and HF morphogenesis initiates, we treated pregnant females with Dox from an earlier time point (E11.5) and initially evaluated the expression of selected, well-established bulge SC markers in the back skin of the offspring at different time points (E14.5, E16.5, and P0) by qRT-PCR. As shown in Fig. 5B, we detected increased transcript levels of *Sox9* (41, 42) at all stages and of *Lhx2* (43, 44) at E14.5 and E16.5 in K14-EPGN mice, while the expression of *Tcf3/4* (34, 45), *Nfatc1* (46), and *Lgr5* (20) remained unchanged. The primary function of LHX2 is to maintain adult HF SCs in an undifferentiated state (44), and it was recently shown that conditional ablation of LHX2 induces sebaceous differentiation in the bulge (47). Thus, it is unlikely that the increased *Lhx2* levels in embryonic skin are responsible for SG hyperplasia in K14-EPGN mice. Most probably, the increased levels of *Lhx2* transcripts are a

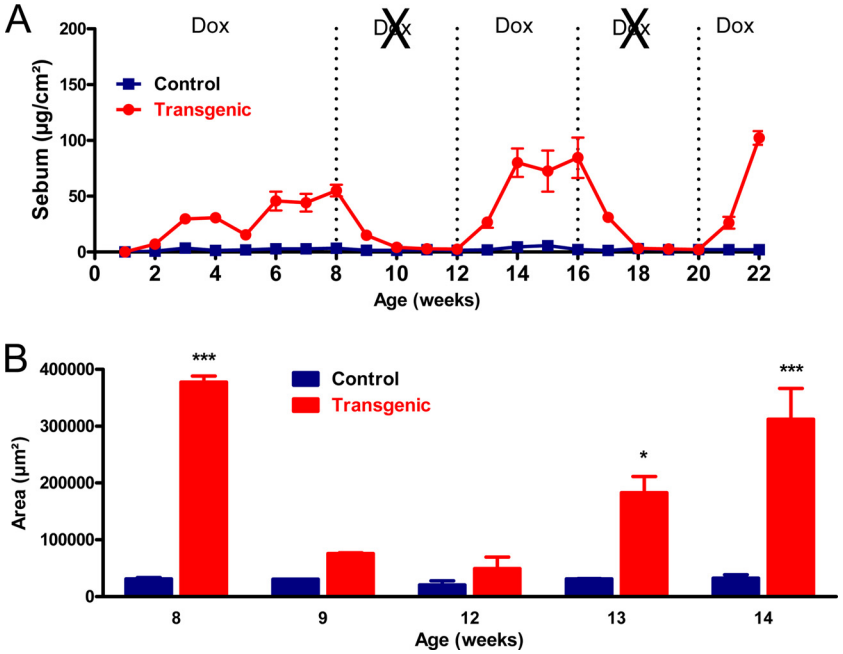

FIG 3 Continuous supply of transgene-derived epigen is necessary for the sebaceous gland phenotype of K14-EPGN mice. (A) Sebum levels of K14-EPGN (Tg) and control (Co) mice were evaluated weekly for 22 weeks with a Sebumeter ($n = 3$ to 6 mice for each genotype). All animals received Dox from E11.5 until postnatal week 8, when Dox was removed from the drinking water for 4 weeks, reintroduced for 4 weeks, removed once more for 4 weeks, and finally added for the last 2 weeks. Differences between genotypes were statistically significant ($P < 0.05$) at all time points except for weeks 1 to 2, 10 to 12, and 18 to 20. (B) Morphometric analysis of sebaceous gland area at the indicated time points endorses the sebum measurements ($n = 3$ mice for each genotype). *, $P < 0.05$; ***, $P < 0.001$.

consequence of the increased HF density in the back skin of K14-EPGN mice, and the same may be true for the increased *Sox9* transcripts. SOX9 is probably the earliest epidermal SC marker, and its expression is restricted to the bulge region in adult skin (41). SOX9 is essential for the morphogenesis of both HF and SG, and its expression can be induced by EGFR signaling (48), making this transcription factor an interesting candidate as a mediator of EPGN actions on the SG. However, epidermal whole mounts of tail skin from P0 or P3 K14-EPGN mice treated with Dox from E11.5 showed no visible changes in the number or distribution of

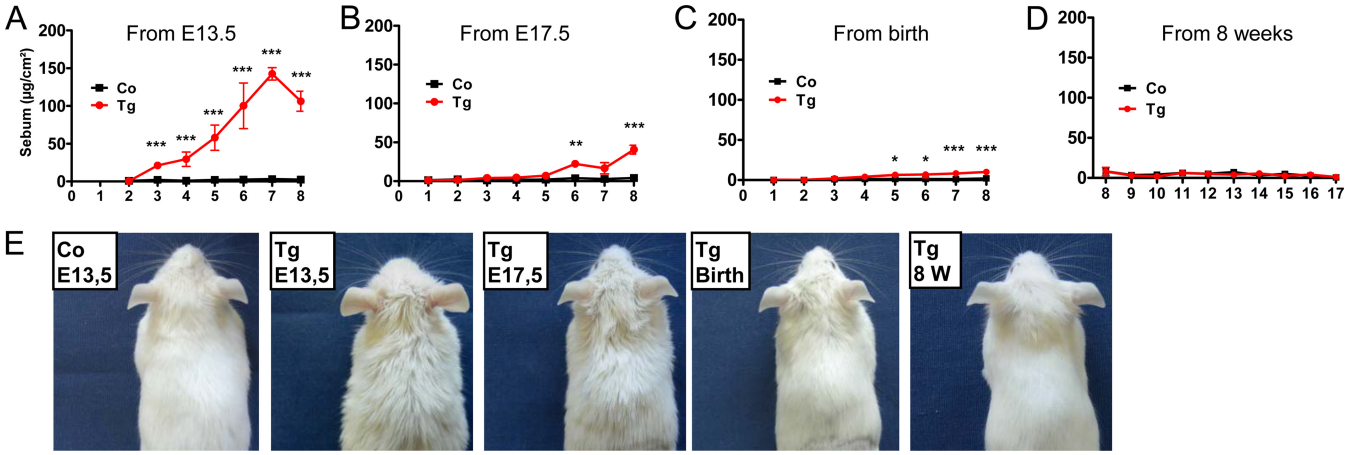

FIG 4 The sebaceous gland phenotype depends on transgene expression before or around the time of epidermal stratification and hair follicle morphogenesis. (A) Exposing K14-EPGN to Dox from E13.5 results in robust increases in postnatal sebum levels, similarly to the exposition from E11.5. Differences between genotypes were statistically significant ($P < 0.05$) from postnatal week 3 ($n = 6$ control and 4 transgenic mice). (B) Exposing K14-EPGN to Dox from E17.5 results in considerably weaker increases in postnatal sebum level. Differences between genotypes were statistically significant ($P < 0.05$) from postnatal week 6 ($n = 5$ control and 5 transgenic mice). (C) Postponing the exposition of K14-EPGN to Dox to the day of birth results in even further decreases in postnatal sebum level. Differences between genotypes were statistically significant ($P < 0.05$) from postnatal week 5 ($n = 10$ control and 6 transgenic mice). (D) When Dox was administered to adult mice (from the 8th week of age), no increases in sebum levels could be observed in K14-EPGN mice ($n = 4$ mice/genotype). (E) Hair coat appearance of 8-week-old control (Co) and K14-EPGN (Tg) receiving Dox from the indicated time points. The rightmost photograph shows a 17-week-old animal. Error bars in panels A to D indicate SEMs. *, $P < 0.05$; **, $P < 0.01$; ***, $P < 0.001$.

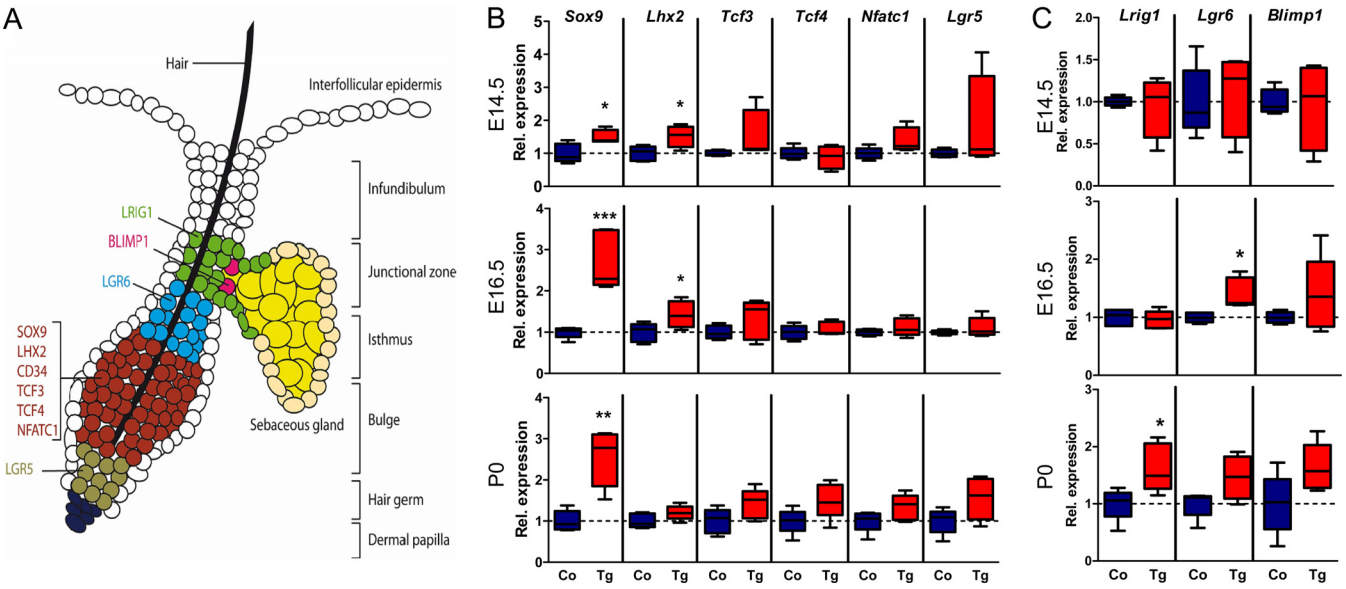

FIG 5 Expression of selected skin stem cell marker transcripts in the back skin of K14-EPGN and control mice. (A) Schematic representation of the stem cell markers evaluated in this study and their locations in the resting (telogen) hair follicle. (B) Transcript levels of the indicated hair follicle bulge stem cell markers in the back skin at E14.5, E16.5, and P0 as evaluated by qRT-PCR ($n = 5$ samples for each genotype). *, $P < 0.05$; **, $P < 0.01$; ***, $P < 0.001$. (C) Transcript levels of the indicated hair follicle isthmus/infundibulum stem cell markers in the back skin at E14.5, E16.5, and P0 as evaluated by qRT-PCR ($n = 5$ samples for each genotype). *, $P < 0.05$.

SOX9-positive cells (see Fig. S2A in the supplemental material). Interestingly, SOX9 was the only SC marker of the pilosebaceous unit with increased expression in the skin of adult mice receiving Dox (even though they do not show any histological skin alteration) (see Fig. S2B), suggesting that while SOX9 expression may be activated by epigen-induced EGFR signaling, its increased levels have little or no consequence for SG growth. Also, no increased levels of the adult bulge SC marker CD34 (14, 49) were detected in the skin of perinatal or adult K14-EPGN mice (data not shown). Thus, our expression analysis data suggest that the bulge precursors do not play a central role in the SG enlargement observed in K14-EPGN mice.

Next, we evaluated known markers of putative sebocyte precursors located in the isthmus or junctional zone of the outer root sheath. Interestingly, these analyses revealed increased levels of *Lrig1* (24) transcripts at P0 and of *Lgr6* (21) transcripts at E16.5, while *Blimp1* (25) levels remained unchanged (Fig. 5C). Although LGR6$^+$ cells can contribute to all epithelial skin compartments, little is known about its regulation, besides the fact that LGR6$^+$ cells appear to reside in a Wnt-independent niche in adult skin (21). Although we cannot exclude an involvement of LGR6 in the SG phenotype, its increased expression may simply reflect the higher HF density in K14-EPGN skin.

In contrast, LRIG1, a transmembrane protein first identified as a keratinocyte SC marker by single-cell expression profiling (50), seems to be a particularly promising candidate for a number of reasons. First, using colocalization of markers, some of us (D. Frances and C. Niemann) recently showed that sebocytes emerge from the LRIG1$^+$ SC compartment during murine SG morphogenesis (28). Second, LRIG1 marks HF SCs that are located in close vicinity to the SG, and lineage tracing has revealed a contribution of LRIG1$^+$ cells to the SG and the infundibulum during homeostasis (24, 51). Third, LRIG1 transcript and protein expression is readily upregulated upon EGFR activation, which is followed by physical association with the EGFR/ERBBs and enhanced receptor ubiquitylation and degradation (52, 53).

Immunofluorescence on whole mounts of tail skin from P0 and P3 K14-EPGN mice receiving Dox from E11.5 demonstrated an expanded pool of LRIG1-positive cells in the upper third of the forming HF (Fig. 6A). To evaluate whether an expanded pool of LRIG1$^+$ cell is maintained in the skin of adult K14-EPGN mice, we measured its expression by qRT-PCR. As shown in Fig. 6B, *Lrig1* transcript levels were significantly increased in the skin of 8-week-old K14-EPGN mice receiving Dox from E11.5 compared to those in control mice. Also, immunofluorescence on histological sections of tail skin (Fig. 6C) revealed that while LRIG1 staining was restricted to a small, discrete group of cells at the opening of the SG in control mice, a considerable larger number of cells around the opening and within the SGs of K14-EPGN mice stained for LRIG1. Furthermore, when Dox was removed from the drinking water of 4-week-old K14-EPGN mice receiving Dox from E11.5, LRIG1 immunoreactivity in K14-EPGN HFs returned to levels comparable to those in control mice; on the other hand, renewed Dox administration for 4 weeks again caused an enlargement of the LRIG1$^+$ pool in the HF of these mice (Fig. 6D), perfectly matching the changes in SG size and sebum output elicited by Dox administration or withdrawal. Thus, our findings indicate that increased EPGN levels expand the LRIG1$^+$ SC population and that the increase in LRIG1 levels may contribute to the enlarged SGs.

The EGFR target gene *Myc* is a positive regulator of LRIG1 expression, both in cultured sebocytes and in mouse skin (24, 50). This is of particular interest given that Myc is a key regulator of epidermal SC commitment to proliferate and differentiate (54). Furthermore, overexpression of MYC in the skin of transgenic

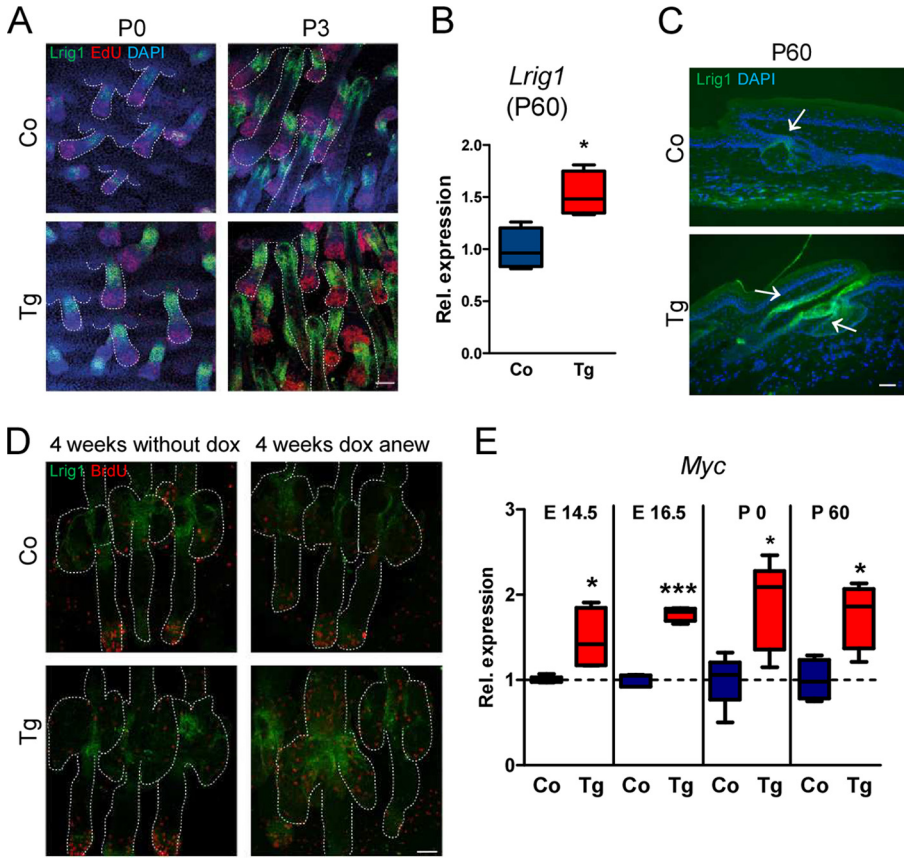

FIG 6 Expression and localization of LRIG1 and Myc in the skin of K14-EPGN (Tg) and control (Co) mice. (A) Immunofluorescence for LRIG1, EdU, and DAPI on epidermal whole-mount preparations showing enlargement of the LRIG1-positive compartment in K14-EPGN (Tg) compared to control (Co) mice at postnatal days 0 and 3. (B) *Lrig1* transcript levels in the back skin of Tg and Co mice at postnatal day 60. (C) Immunofluorescence for LRIG1 and DAPI on histological sections of tail skin showing enlargement of the LRIG1-positive compartment (arrows) in Tg mice at postnatal day 60. (D) Immunofluorescence for LRIG1 and bromodeoxyuridine (BrdU) on epidermal whole-mount preparations in mice of the indicated genotypes and receiving Dox from E11.5 at 8 weeks of age (4 weeks without Dox before death) or 12 weeks of age (4 weeks Dox anew). (E) *Myc* transcript levels in the back skin of Tg and Co mice at the indicated embryonic or postnatal stages. For panels B and E, 5 samples were used for each genotype. *, $P < 0.05$; ***, $P < 0.001$. Scale bars represent 50 μm.

mice results in SG enlargement (55, 56). In addition, increased *Myc* expression was previously detected in the skin of Dsk5 mice, a mutant line expressing a constitutively active EGFR that also exhibits enlarged SGs (57). To evaluate a possible involvement of Myc in the SG phenotype of K14-EPGN mice, we therefore measured its expression by qRT-PCR. As shown in Fig. 6E, significantly increased *Myc* expression was seen in K14-EPGN back skin of mice receiving Dox from E11.5 at E14.5, E16.5, and P0. Also, similarly to *Lrig1*, the expression of *Myc* in the skin of 8-week-old K14-EPGN mice receiving Dox from E11.5 was significantly increased compared to that of control mice (Fig. 6E).

DISCUSSION

It has long been known that the transmembrane protein LRIG1 negatively regulates EGFR/ERBB signaling by mediating ubiquitination and degradation of activated receptors (52, 53). More recently, LRIG1 was also identified as a marker for adult SCs in organs such as the skin (24, 50, 51) and intestine (58, 59). While a role for LRIG1 in maintaining intestinal SC quiescence by calibrating ERBB signaling was recently suggested (58, 59), such a functional relationship has not been shown for skin SCs so far.

In this study, using a transgenic mouse line with tissue-specific and inducible expression of the EGFR ligand epigen, we showed that activation of the EGFR by its ligand epigen during early epidermal development causes hyperplasia of the SGs and, to a minor extent, hyperplasia of the IFE and increased HF density. The increased HF density represents an intriguing finding that deserves further investigation, but it was not the focus of this study. The SG enlargement, which is EGFR dependent and can be reversed by withdrawal of epigen, is associated with an expanded pool of LRIG1$^+$ cells located in the junctional zone, the region around the SG opening. Since such a regulation of SG size and output by Dox administration to K14-EPGN mice was not achieved when the treatment is initiated postnatally, the early excess of epigen seems to influence the HF LRIG1$^+$ cells by an unknown mechanism, rendering them susceptible for later increases in EPGN/EGFR signaling.

We also detected parallel increased *Myc* expression in the skin of transgenic mice, suggesting that once established, the LRIG1$^+$ pool can offer a large number of proliferating, MYC$^+$ progenitor cells that contribute to the expanded SG and IFE lineages under EGFR-dependent mitogenic stimuli. These results shed light on

the relationship between EGFR/ERBBs and LRIG1 and support a model in which the commitment of SCs toward specific progenitor cells is regulated by the reciprocal interaction of these proteins. Considering the actions of LRIG1 as an SC marker, tumor suppressor, and ERBB negative regulator (60), our findings also have implications for skin neoplastic diseases.

ACKNOWLEDGMENTS

We thank M. Wegner (University of Erlangen) for providing the SOX9 antibody.

This work was supported by a grant from the Deutsche Forschungsgemeinschaft (DFG) to M.R.S. (SCHN1081/3-1). C.N. acknowledges support from the DFG (project A3 SFB 829).

We declare no potential conflicts of interest.

REFERENCES

1. **Beck B, Blanpain C.** 2012. Mechanisms regulating epidermal stem cells. EMBO J. **31:**2067–2075. http://dx.doi.org/10.1038/emboj.2012.67.
2. **Goldstein J, Horsley V.** 2012. Home sweet home: skin stem cell niches. Cell Mol. Life Sci. **69:**2573–2582. http://dx.doi.org/10.1007/s00018-012-0943-3.
3. **Jaks V, Kasper M, Toftgard R.** 2010. The hair follicle—a stem cell zoo. Exp. Cell Res. **316:**1422–1428. http://dx.doi.org/10.1016/j.yexcr.2010.03.014.
4. **Rompolas P, Greco V.** 2014. Stem cell dynamics in the hair follicle niche. Semin. Cell Dev. Biol. **25-26:**34–42. http://dx.doi.org/10.1016/j.semcdb.2013.12.005.
5. **Tumbar T.** 31 January 2012. Ontogeny and homeostasis of adult epithelial skin stem cells. Stem Cell Rev. http://dx.doi.org/10.1007/s12015-012-9348-9.
6. **Mascré G, Dekoninck S, Drogat B, Youssef KK, Brohee S, Sotiropoulou PA, Simons BD, Blanpain C.** 2012. Distinct contribution of stem and progenitor cells to epidermal maintenance. Nature **489:**257–262. http://dx.doi.org/10.1038/nature11393.
7. **Jones PH, Simons BD, Watt FM.** 2007. Sic transit gloria: farewell to the epidermal transit amplifying cell? Cell Stem Cell **1:**371–381. http://dx.doi.org/10.1016/j.stem.2007.09.014.
8. **Alonso L, Fuchs E.** 2006. The hair cycle. J. Cell Sci. **119:**391–393. http://dx.doi.org/10.1242/jcs02793.
9. **Schneider MR, Schmidt-Ullrich R, Paus R.** 2009. The hair follicle as a dynamic miniorgan. Curr. Biol. **19:**R132–R142. http://dx.doi.org/10.1016/j.cub.2008.12.005.
10. **Sennett R, Rendl M.** 2012. Mesenchymal-epithelial interactions during hair follicle morphogenesis and cycling. Semin. Cell Dev. Biol. **23:**917–927. http://dx.doi.org/10.1016/j.semcdb.2012.08.011.
11. **Cotsarelis G, Sun TT, Lavker RM.** 1990. Label-retaining cells reside in the bulge area of pilosebaceous unit: implications for follicular stem cells, hair cycle, and skin carcinogenesis. Cell **61:**1329–1337. http://dx.doi.org/10.1016/0092-8674(90)90696-C.
12. **Liu Y, Lyle S, Yang Z, Cotsarelis G.** 2003. Keratin 15 promoter targets putative epithelial stem cells in the hair follicle bulge. J. Invest. Dermatol. **121:**963–968. http://dx.doi.org/10.1046/j.1523-1747.2003.12600.x.
13. **Lyle S, Christofidou-Solomidou M, Liu Y, Elder DE, Albelda S, Cotsarelis G.** 1998. The C8/144B monoclonal antibody recognizes cytokeratin 15 and defines the location of human hair follicle stem cells. J. Cell Sci. **111**(Part 21)**:**3179–3188.
14. **Trempus CS, Morris RJ, Bortner CD, Cotsarelis G, Faircloth RS, Reece JM, Tennant RW.** 2003. Enrichment for living murine keratinocytes from the hair follicle bulge with the cell surface marker CD34. J. Invest. Dermatol. **120:**501–511. http://dx.doi.org/10.1046/j.1523-1747.2003.12088.x.
15. **Morris RJ, Liu Y, Marles L, Yang Z, Trempus C, Li S, Lin JS, Sawicki JA, Cotsarelis G.** 2004. Capturing and profiling adult hair follicle stem cells. Nat. Biotechnol. **22:**411–417. http://dx.doi.org/10.1038/nbt950.
16. **Petersson M, Brylka H, Kraus A, John S, Rappl G, Schettina P, Niemann C.** 2011. TCF/Lef1 activity controls establishment of diverse stem and progenitor cell compartments in mouse epidermis. EMBO J. **30:**3004–3018. http://dx.doi.org/10.1038/emboj.2011.199.
17. **Ito M, Liu Y, Yang Z, Nguyen J, Liang F, Morris RJ, Cotsarelis G.** 2005. Stem cells in the hair follicle bulge contribute to wound repair but not to homeostasis of the epidermis. Nat. Med. **11:**1351–1354. http://dx.doi.org/10.1038/nm1328.
18. **Taylor G, Lehrer MS, Jensen PJ, Sun TT, Lavker RM.** 2000. Involvement of follicular stem cells in forming not only the follicle but also the epidermis. Cell **102:**451–461. http://dx.doi.org/10.1016/S0092-8674(00)00050-7.
19. **Tumbar T, Guasch G, Greco V, Blanpain C, Lowry WE, Rendl M, Fuchs E.** 2004. Defining the epithelial stem cell niche in skin. Science **303:**359–363. http://dx.doi.org/10.1126/science.1092436.
20. **Jaks V, Barker N, Kasper M, van Es JH, Snippert HJ, Clevers H, Toftgard R.** 2008. Lgr5 marks cycling, yet long-lived, hair follicle stem cells. Nat. Genet. **40:**1291–1299. http://dx.doi.org/10.1038/ng.239.
21. **Snippert HJ, Haegebarth A, Kasper M, Jaks V, van Es JH, Barker N, van de Wetering M, van den Born M, Begthel H, Vries RG, Stange DE, Toftgard R, Clevers H.** 2010. Lgr6 marks stem cells in the hair follicle that generate all cell lineages of the skin. Science **327:**1385–1389. http://dx.doi.org/10.1126/science.1184733.
22. **Nijhof JG, Braun KM, Giangreco A, van Pelt C, Kawamoto H, Boyd RL, Willemze R, Mullenders LH, Watt FM, de Gruijl FR, van Ewijk W.** 2006. The cell-surface marker MTS24 identifies a novel population of follicular keratinocytes with characteristics of progenitor cells. Development **133:**3027–3037. http://dx.doi.org/10.1242/dev.02443.
23. **Raymond K, Richter A, Kreft M, Frijns E, Janssen H, Slijper M, Praetzel-Wunder S, Langbein L, Sonnenberg A.** 2010. Expression of the orphan protein Plet-1 during trichilemmal differentiation of anagen hair follicles. J. Invest. Dermatol. **130:**1500–1513. http://dx.doi.org/10.1038/jid.2010.4.
24. **Jensen KB, Collins CA, Nascimento E, Tan DW, Frye M, Itami S, Watt FM.** 2009. Lrig1 expression defines a distinct multipotent stem cell population in mammalian epidermis. Cell Stem Cell **4:**427–439. http://dx.doi.org/10.1016/j.stem.2009.04.014.
25. **Horsley V, O'Carroll D, Tooze R, Ohinata Y, Saitou M, Obukhanych T, Nussenzweig M, Tarakhovsky A, Fuchs E.** 2006. Blimp1 defines a progenitor population that governs cellular input to the sebaceous gland. Cell **126:**597–609. http://dx.doi.org/10.1016/j.cell.2006.06.048.
26. **Niemann C, Horsley V.** 2012. Development and homeostasis of the sebaceous gland. Semin. Cell Dev. Biol. **23:**928–936. http://dx.doi.org/10.1016/j.semcdb.2012.08.010.
27. **Schneider MR, Paus R.** 2010. Sebocytes, multifaceted epithelial cells: lipid production and holocrine secretion. Int. J. Biochem. Cell Biol. **42:**181–185. http://dx.doi.org/10.1016/j.biocel.2009.11.017.
28. **Frances D, Niemann C.** 2012. Stem cell dynamics in sebaceous gland morphogenesis in mouse skin. Dev. Biol. **363:**138–146. http://dx.doi.org/10.1016/j.ydbio.2011.12.028.
29. **Panteleyev AA, Rosenbach T, Paus R, Christiano AM.** 2000. The bulge is the source of cellular renewal in the sebaceous gland of mouse skin. Arch. Dermatol. Res. **292:**573–576. http://dx.doi.org/10.1007/s004030000182.
30. **Dahlhoff M, Muller AK, Wolf E, Werner S, Schneider MR.** 2010. Epigen transgenic mice develop enlarged sebaceous glands. J. Invest. Dermatol. **130:**623–626. http://dx.doi.org/10.1038/jid.2009.251.
31. **Schneider MR, Wolf E.** 2009. The epidermal growth factor receptor ligands at a glance. J. Cell Physiol. **218:**460–466. http://dx.doi.org/10.1002/jcp.21635.
32. **Schneider MR, Yarden Y.** 2014. Structure and function of epigen, the last EGFR ligand. Semin. Cell Dev. Biol. **28:**57–61. http://dx.doi.org/10.1016/j.semcdb.2013.12.011.
33. **Lee D, Cross SH, Strunk KE, Morgan JE, Bailey CL, Jackson IJ, Threadgill DW.** 2004. Wa5 is a novel ENU-induced antimorphic allele of the epidermal growth factor receptor. Mamm. Genome **15:**525–536. http://dx.doi.org/10.1007/s00335-004-2384-2.
34. **Nguyen H, Rendl M, Fuchs E.** 2006. Tcf3 governs stem cell features and represses cell fate determination in skin. Cell **127:**171–183. http://dx.doi.org/10.1016/j.cell.2006.07.036.
35. **Paus R, Muller-Rover S, Van DV, Maurer M, Eichmuller S, Ling G, Hofmann U, Foitzik K, Mecklenburg L, Handjiski B.** 1999. A comprehensive guide for the recognition and classification of distinct stages of hair follicle morphogenesis. J. Invest. Dermatol. **113:**523–532. http://dx.doi.org/10.1046/j.1523-1747.1999.00740.x.
36. **Müller-Röver S, Handjiski B, Van DV, Eichmuller S, Foitzik K, McKay IA, Stenn KS, Paus R.** 2001. A comprehensive guide for the accurate classification of murine hair follicles in distinct hair cycle stages. J. Invest. Dermatol. **117:**3–15. http://dx.doi.org/10.1046/j.0022-202x.2001.01377.x.
37. **Stolt CC, Lommes P, Sock E, Chaboissier MC, Schedl A, Wegner M.** 2003. The Sox9 transcription factor determines glial fate choice in the

developing spinal cord. Genes Dev. **17:**1677–1689. http://dx.doi.org/10.1101/gad.259003.

38. **Hinde E, Haslam IS, Schneider MR, Langan EA, Kloepper JE, Schramm C, Zouboulis CC, Paus R.** 2013. A practical guide for the study of human and murine sebaceous glands in situ. Exp. Dermatol. **22:**631–637. http://dx.doi.org/10.1111/exd.12207.
39. **Kiguchi K, Bol D, Carbajal S, Beltran L, Moats S, Chan K, Jorcano J, Digiovanni J.** 2000. Constitutive expression of erbB2 in epidermis of transgenic mice results in epidermal hyperproliferation and spontaneous skin tumor development. Oncogene **19:**4243–4254. http://dx.doi.org/10.1038/sj.onc.1203778.
40. **Ghazizadeh S, Taichman LB.** 2001. Multiple classes of stem cells in cutaneous epithelium: a lineage analysis of adult mouse skin. EMBO J. **20:**1215–1222. http://dx.doi.org/10.1093/emboj/20.6.1215.
41. **Nowak JA, Polak L, Pasolli HA, Fuchs E.** 2008. Hair follicle stem cells are specified and function in early skin morphogenesis. Cell Stem Cell **3:**33–43. http://dx.doi.org/10.1016/j.stem.2008.05.009.
42. **Vidal VP, Chaboissier MC, Lutzkendorf S, Cotsarelis G, Mill P, Hui CC, Ortonne N, Ortonne JP, Schedl A.** 2005. Sox9 is essential for outer root sheath differentiation and the formation of the hair stem cell compartment. Curr. Biol. **15:**1340–1351. http://dx.doi.org/10.1016/j.cub.2005.06.064.
43. **Mardaryev AN, Ahmed MI, Vlahov NV, Fessing MY, Gill JH, Sharov AA, Botchkareva NV.** 2010. Micro-RNA-31 controls hair cycle-associated changes in gene expression programs of the skin and hair follicle. FASEB J. **24:**3869–3881. http://dx.doi.org/10.1096/fj.10-160663.
44. **Rhee H, Polak L, Fuchs E.** 2006. Lhx2 maintains stem cell character in hair follicles. Science **312:**1946–1949. http://dx.doi.org/10.1126/science.1128004.
45. **Nguyen H, Merrill BJ, Polak L, Nikolova M, Rendl M, Shaver TM, Pasolli HA, Fuchs E.** 2009. Tcf3 and Tcf4 are essential for long-term homeostasis of skin epithelia. Nat. Genet. **41:**1068–1075. http://dx.doi.org/10.1038/ng.431.
46. **Horsley V, Aliprantis AO, Polak L, Glimcher LH, Fuchs E.** 2008. NFATc1 balances quiescence and proliferation of skin stem cells. Cell **132:**299–310. http://dx.doi.org/10.1016/j.cell.2007.11.047.
47. **Folgueras AR, Guo X, Pasolli HA, Stokes N, Polak L, Zheng D, Fuchs E.** 2013. Architectural niche organization by LHX2 is linked to hair follicle stem cell function. Cell Stem Cell **13:**314–327. http://dx.doi.org/10.1016/j.stem.2013.06.018.
48. **Ling S, Chang X, Schultz L, Lee TK, Chaux A, Marchionni L, Netto GJ, Sidransky D, Berman DM.** 2011. An EGFR-ERK-SOX9 signaling cascade links urothelial development and regeneration to cancer. Cancer Res. **71:**3812–3821. http://dx.doi.org/10.1158/0008-5472.CAN-10-3072.
49. **Blanpain C, Lowry WE, Geoghegan A, Polak L, Fuchs E.** 2004. Self-renewal, multipotency, and the existence of two cell populations within an epithelial stem cell niche. Cell **118:**635–648. http://dx.doi.org/10.1016/j.cell.2004.08.012.
50. **Jensen KB, Watt FM.** 2006. Single-cell expression profiling of human epidermal stem and transit-amplifying cells: Lrig1 is a regulator of stem cell quiescence. Proc. Natl. Acad. Sci.U. S. A. **103:**11958–11963. http://dx.doi.org/10.1073/pnas.0601886103.
51. **Page ME, Lombard P, Ng F, Gottgens B, Jensen KB.** 2013. The epidermis comprises autonomous compartments maintained by distinct stem cell populations. Cell Stem Cell **13:**471–482. http://dx.doi.org/10.1016/j.stem.2013.07.010.
52. **Gur G, Rubin C, Katz M, Amit I, Citri A, Nilsson J, Amariglio N, Henriksson R, Rechavi G, Hedman H, Wides R, Yarden Y.** 2004. LRIG1 restricts growth factor signaling by enhancing receptor ubiquitylation and degradation. EMBO J. **23:**3270–3281. http://dx.doi.org/10.1038/sj.emboj.7600342.
53. **Laederich MB, Funes-Duran M, Yen L, Ingalla E, Wu X, Carraway KL III, Sweeney C.** 2004. The leucine-rich repeat protein LRIG1 is a negative regulator of ErbB family receptor tyrosine kinases. J. Biol. Chem. **279:**47050–47056. http://dx.doi.org/10.1074/jbc.M409703200.
54. **Gandarillas A, Watt FM.** 1997. c-Myc promotes differentiation of human epidermal stem cells. Genes Dev. **11:**2869–2882. http://dx.doi.org/10.1101/gad.11.21.2869.
55. **Arnold I, Watt FM.** 2001. c-Myc activation in transgenic mouse epidermis results in mobilization of stem cells and differentiation of their progeny. Curr. Biol. **11:**558–568. http://dx.doi.org/10.1016/S0960-9822(01)00154-3.
56. **Waikel RL, Kawachi Y, Waikel PA, Wang XJ, Roop DR.** 2001. Deregulated expression of c-Myc depletes epidermal stem cells. Nat. Genet. **28:**165–168. http://dx.doi.org/10.1038/88889.
57. **Dahlhoff M, de Angelis MH, Wolf E, Schneider MR.** 2013. Ligand-independent epidermal growth factor receptor hyperactivation increases sebaceous gland size and sebum secretion in mice. Exp. Dermatol. **22:**667–669. http://dx.doi.org/10.1111/exd.12219.
58. **Powell AE, Wang Y, Li Y, Poulin EJ, Means AL, Washington MK, Higginbotham JN, Juchheim A, Prasad N, Levy SE, Guo Y, Shyr Y, Aronow BJ, Haigis KM, Franklin JL, Coffey RJ.** 2012. The pan-ErbB negative regulator Lrig1 is an intestinal stem cell marker that functions as a tumor suppressor. Cell **149:**146–158. http://dx.doi.org/10.1016/j.cell.2012.02.042.
59. **Wong VW, Stange DE, Page ME, Buczacki S, Wabik A, Itami S, WMvan de, Poulsom R, Wright NA, Trotter MW, Watt FM, Winton DJ, Clevers H, Jensen KB.** 2012. Lrig1 controls intestinal stem-cell homeostasis by negative regulation of ErbB signalling. Nat. Cell Biol. **14:**401–408. http://dx.doi.org/10.1038/ncb2464.
60. **Wang Y, Poulin EJ, Coffey RJ.** 2013. LRIG1 is a triple threat: ERBB negative regulator, intestinal stem cell marker and tumour suppressor. Br. J. Cancer **108:**1765–1770. http://dx.doi.org/10.1038/bjc.2013.138.